

Coulomb gap in a doped semiconductor near the metal-insulator transition: Tunneling experiment and scaling ansatz

Mark Lee* and J. G. Massey

Department of Physics, University of Virginia, Charlottesville, Virginia 22903

V. L. Nguyen and B. I. Shklovskii

Theoretical Physics Institute, University of Minnesota, Minneapolis, Minnesota 55455

(Received 30 December 1998)

Electron tunneling experiments are used to probe Coulomb correlation effects in the single-particle density of states (DOS) of boron-doped silicon crystals near the critical density n_c of the metal-insulator transition (MIT). At low energies ($\epsilon \leq 0.5$ meV), a DOS measurement distinguishes between insulating and metallic samples with densities 10 to 15 % on either side of n_c . However, at higher energies (~ 1 meV $\leq \epsilon \leq 50$ meV) the DOS of both insulators and metals show a common behavior, increasing with energy as ϵ^m where m is roughly 0.5. The observed characteristics of the DOS can be understood using a classical treatment of Coulomb interactions combined with a phenomenological scaling ansatz to describe the length-scale dependence of the dielectric constant as the MIT is approached from the insulating side. [S0163-1829(99)12427-5]

I. INTRODUCTION

Since 1979 the best available description of the disorder-driven metal-insulator transition (MIT) has been based on the noninteracting scaling theory of Abrahams *et al.*¹ Although it treats thoroughly the localizing effects of electron scattering off static disorder, this theory is incomplete because it neglects electron-electron interactions. In particular, below the critical density n_c of the MIT the vanishing carrier mobility means that Coulomb correlations are strong enough to warrant treatment on equal footing with the disorder. The importance of interactions is illustrated by several well-known, apparently anomalous phenomena,² such as the recent discovery by Kravchenko *et al.*^{3,4} of a “forbidden” metallic state in a two-dimensional (2D) electron system. In a disordered metal, electron-electron interactions lead to a singular negative correction to the single-particle density of states (DOS) near the Fermi level.⁵ Deep into the insulating side, it is well established that Coulomb correlations cause a Coulomb gap in the DOS near the Fermi level, which changes the temperature dependence of the dc electrical conductivity at very low temperatures.^{6,7} How these two renormalizations of the DOS evolve in the critical region of the MIT and match each other at n_c is one of the most challenging and long-standing questions of solid-state physics.

Combining both disorder and Coulomb interactions into a unified scaling description of disordered metals near the MIT was attempted by McMillan⁸ and by Gefen and Imry.⁹ These models were criticized¹⁰ for the use of the single-particle, rather than thermodynamic, DOS in describing the charge screening, as discussed in detail in Sec. III, and have not been widely accepted despite garnering some experimental support.¹¹ Later renormalization group theories by Finkelstein,¹² Castellani *et al.*,¹³ and Kirkpatrick and Belitz¹⁴ used a Fermi-liquid-based approach to describe the diffusion of interacting quasiparticles in a disordered metal. These works employed a smooth thermodynamic DOS (or compressibility) and started from perturbative treatments of weak

disorder. All agree with the basic findings of Altshuler and Aronov⁵ (AA) that there should be a square-root (in 3D) or logarithmic (in 2D) depletion in the single-particle DOS at the Fermi level of a disordered metal. However, they failed to generate a well-defined, continuous charge-localization transition at nonzero disorder and finite interaction strength, and cannot describe the emergence of a Coulomb glass state and the Coulomb gap as a system crosses over into the insulating state.

Tunneling experiments have observed AA-like depletions in the DOS of a variety of disordered metals, including amorphous metal-semiconductor alloys,^{15,16,11} doped semiconductors,¹⁷ and granular metals.¹⁸ By contrast, with the exception of the singular sodium tungsten bronze system,¹⁹ the existence of the Coulomb gap in localized insulators has until recently been only indirectly inferred from activation fits to dc conductivity²⁰ or relaxation measurements.²¹ Only in the last few years have quantitative tunneling spectroscopic observations of the Coulomb gap been made in 3D (Refs. 22 and 23) and in 2D (Ref. 24) nonmetallic semiconductors.

Most previous work on interaction effects has emphasized the metallic side; much less corresponding effort, experimental or theoretical, exists to describe the insulating side near the critical region of the MIT. The important role long-range Coulomb interactions play in affecting the empirical scaling characteristics of the complex ac conductivity as the MIT is approached from below was emphasized by Paalanen *et al.*²⁵ in stress-tuning experiments on phosphorous-doped silicon. In this paper, we concentrate on studying directly the Coulomb gap in the DOS that occurs in 3D disordered insulators close to the MIT. Results of tunneling measurements of the DOS in boron-doped silicon are presented over a much larger range of energies than in Refs. 22 and 23. The tunneling DOS spectra show that metals and insulators can be distinguished by the low-energy characteristics of the DOS (i.e., square-root cusp vs parabolic Coulomb gap), but that metals and insulators share a common, roughly square-root high-

energy DOS behavior that is approximately independent of dopant densities close to n_c . Of course, a truly complete microscopic theory of the MIT with interactions should cover the continuous crossover from insulating to metallic state. We present a much more modest and simple scaling approach to the MIT, which emphasizes the insulating side and is based on an extension of the Efros-Shklovskii⁶ arguments. Using the idea of a dielectric constant with spatial dispersion,^{8,9} we argue that at the point of the MIT a power-law depletion of the DOS near the Fermi level is still the Efros-Shklovskii (ES) Coulomb gap, only modified by this dispersion. The scaling ansatz describes well the main features of the experimental data.

This paper is organized as follows: Sec. II presents experimental details and data, Sec. III develops the scaling description, and Sec. IV analyzes of the data with respect to the scaling model.

II. TUNNELING MEASUREMENTS OF THE COULOMB GAP

When a conductor is separated from a conventional metal by a rectangular potential barrier high enough to prevent classical current flow but thin enough to permit quantum tunneling, the tunneling conductance at temperature T , $G(V, T) = dI/dV$ where I is the tunneling current and V is the voltage bias across the junction, is given by²⁶

$$\frac{G(V)}{G_0} = \int \frac{N(\varepsilon)}{N_0} \frac{\partial f(\varepsilon - eV, T)}{\partial eV} d\varepsilon, \quad (2.1)$$

where G_0 is the conductance in the noninteracting case, $N(\varepsilon, T)/N_0$ is the interacting single-particle DOS relative to the noninteracting value N_0 , and f is the Fermi function. We take the zero of energy at $\varepsilon_F = 0$. The highest bias used in this experiment is 50 meV, which is much smaller than the several eV height of the SiO_2 barrier, so that the barrier transmission coefficient is taken to be independent of bias. In nearly all tunneling measurements, the normalizing conductance G_0 is taken at a relatively high-voltage bias, where $G(V)$ is either constant or only slowly varying on the energy scale of the spectral features of interest. The normalized conductance then gives the ratio $N(eV, T)/N_0$, thermally broadened by convolution with $-\partial f/\partial(eV)$. At sufficiently low temperature, when $k_B T$ is much smaller than the energy scale of characteristic variations in $N(\varepsilon)$, ordinary thermal broadening can be neglected so that $G(V, T)/G_0$ is directly proportional to $N(eV, T)/N_0$. Note that, unlike the noninteracting case, $N(eV, T)$ can have a nontrivial intrinsic temperature dependence separate from ordinary thermal broadening.

The Si:B crystals used were characterized by measuring their room-temperature resistivities ρ and resistivity ratios (RR's) $\rho(4.2\text{K})/\rho(300\text{K})$. Dopant densities n were obtained using the calibration of Thurber *et al.*²⁷ and the data of Dai *et al.*²⁸ to translate between measured RR's and dopant densities. Samples used had RR's of 2.3 to 18, corresponding to n/n_c of 110% to 81%, respectively, where we take²⁸ $n_c = 4.0 \times 10^{18} \text{ cm}^{-3}$. Details of the dc variable-range hopping (VRH) conductivity in many of these samples have been published previously.^{22,29} The static dielectric constants

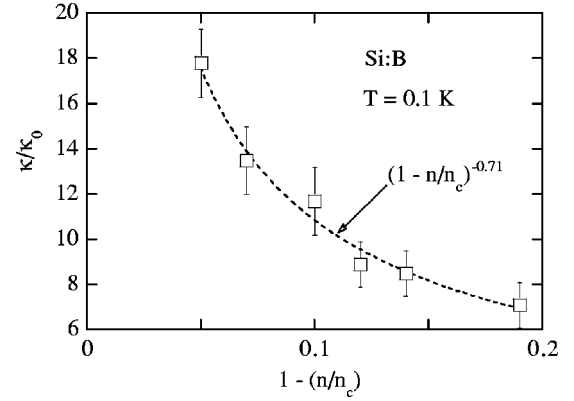


FIG. 1. Static dielectric constants (in units of the Si dielectric constant $\kappa_0 = 11.7$) as a function of the normalized dopant density for a set of insulating Si:B crystals. These data were measured at a temperature $T = 0.1$ K. The solid curve is a fit to the functional form $\kappa(n/n_c) \sim (1 - n/n_c)^{-\zeta}$, which gives $\zeta \approx 0.71$.

of several insulating crystals were measured using a capacitance method similar to that described by Castner.³⁰ These results are shown in Fig. 1. To compare values with the literature, on an 86% sample we obtained $\kappa/\kappa_0 = 8.5 \pm 1$, where $\kappa_0 = 11.7$ is the dielectric constant of the host Si lattice. This value is in reasonable agreement with published values^{25,31} on Si:As and Si:P at similar values of n/n_c . The curve in Fig. 1 is a fit of the data to $\kappa(n) \sim (1 - n/n_c)^{-\zeta}$, which yields $\zeta \approx 0.71$.

Tunnel junctions were formed by creating a very thin (estimated 15 to 30 Å) layer of SiO_2 as a tunnel barrier on the Si:B crystals, and using an Al film as the counter-electrode. Details of the fabrication of these metal-oxide-semiconductor structures were described previously. The major modification from the prior description was the use of an ultraviolet ozone method in place of a chemical oxide growth to clean the silicon surfaces and produce more reproducible ultrathin SiO_2 tunnel barriers. SiO_2 thicknesses were estimated from published calibrations of UV exposure time, temperature, and O_2 flow rate.³² Good junctions were those that showed a signature of the Al superconducting energy gap below 1 K. These devices had junction resistances between 65 to 850 kΩ near 1 K.

Tunneling current-voltage ($I-V$) and conductance-voltage [$G(V)$] traces were taken using standard analog methods. Where required, a small (1 kG) magnetic field was used to suppress the superconductivity in the Al electrode. We shall refer to such data as “zero Teslas.” Data down to 1.2 K were obtained by suspending the samples stress free from their leads and immersing in a pumped liquid ^4He bath. To reach lower temperatures, the samples were immersed in the $^3\text{He}/^4\text{He}$ mixture of a dilution refrigerator. Cooling power at 0.1 K was measured to be 120 μW , while no more than 0.1 μW of power was used to take the data. Temperature stability of better than 1 mK at 1.2 K and 0.1 mK at 0.1 K could be obtained, which was important to prevent thermal fluctuations from coupling to the highly temperature-dependent resistance in the more insulating samples. For samples with $n/n_c > 90\%$, reliable data could be taken below 0.1 K. For insulating samples with $n/n_c < 90\%$, the resistance of the Si:B crystal itself rose to exceed 10% of the resistance across the tunnel junction below 0.1 K. Because

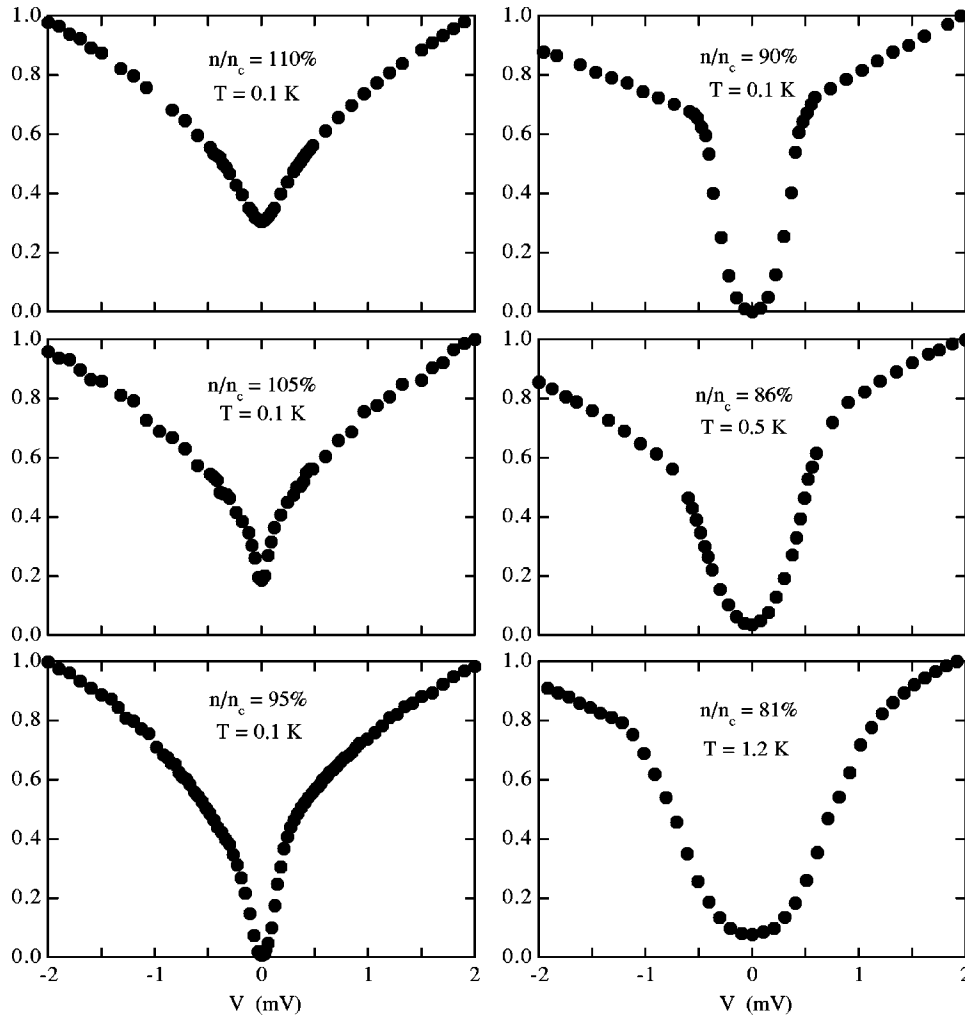


FIG. 2. Low-bias tunneling conductance-voltage spectra for Si:B samples at several different values of n/n_c . All data sets are normalized to the conductance at +2 mV. Data for samples with $n/n_c \geq 90\%$ were taken at $T=0.1$ K. Data for the 86 and 81 % samples were taken at 0.5 and 1.2 K, respectively.

the crystal acted as a voltage drop in series with the junction, quantitative tunneling conductance data below ~ 0.1 K is not reliable in these most insulating samples. Therefore, we present only $T \geq 0.5$ K data for these samples, where the voltage drop across the Si:B crystal is no more than a 1% correction to the tunnel junction conductance.

Figure 2 shows low-energy tunneling conductance spectra on six samples with densities $n/n_c = 81, 86, 90, 95, 105,$ and 110% , all in zero Teslas. All data are normalized to the conductance value of each sample at +2 mV. The spectrum for the 81% sample was taken at 1.2 K, the spectrum for the 86% sample was taken at 0.5 K, and the data for the other four samples were taken at 0.1 K. Ordinary thermal broadening at the measurement temperatures is minor compared to the energy scale of the conductance features, and so has not been deconvoluted from the data. However, the interacting DOS of each sample has an intrinsic finite-temperature dependence that may be more obvious in the data for the 81 and 86% samples because of the higher temperature. In the conductance spectra, there is a clear difference between the insulating and metallic samples at low biases, $|V| < 1$ mV. In all the insulating samples, a conductance dip across zero voltage (the Fermi level in tunneling measurements) is the signature of the Coulomb gap. For the 81 and 86% samples,

$G(V=0)$ is small but greater than zero because the measurement temperature for these two samples is sufficiently high that there is some intrinsic filling in of the $T=0$ gap. In all insulating samples, the low-energy conductance spectra fit a power-law form $N(\varepsilon) \propto |\varepsilon|^p$ with $p = 2.4, 2.2, 2.2,$ and 2.0 for the 81, 86, 90, and 95 % samples, respectively, at the (different) measurement temperatures. As $n \rightarrow n_c$ from below, the gap sides steepen and the width of the Coulomb gap around zero bias narrows. Although the gap ‘‘shoulders’’ are soft and therefore not precisely definable, the approximate full width δ of the parabolic-like ($p \approx 2$) gap is about 2.2, 1.5, 1.1, and 0.6 mV and for the 81, 86, 90, and 95 % samples, respectively. By contrast, both the metallic samples show a significantly large nonzero conductance at $V=0$, with a sharp dip³³ around zero bias that is well fit to a square-root form $N(\varepsilon) = N(0)[1 + (|\varepsilon|/\delta)^2]^{1/2}$ at low bias. Fits to this form give $\delta \approx 0.25$ and 0.4 meV for the 110 and 105% samples, respectively. Normalizing the metallic data to $G(+50 \text{ mV})$, the ratio of zero-bias conductances is $G_{110}(0)/G_{105}(0) = 1.7$, so that the more metallic sample has a larger DOS at the Fermi level, as expected.

Figure 3 compares tunneling conductance spectra over an extended bias range (0.03 to 50 mV) for two metallic and

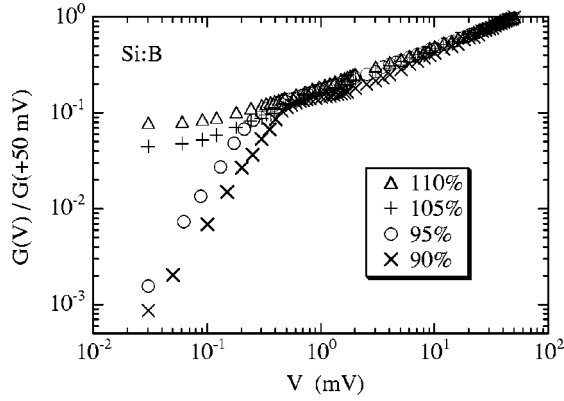


FIG. 3. Extended bias range tunneling conductance spectra for four Si:B samples, two metallic (110 and 105 %) and two insulating (95 and 90 %), all taken at temperature $T=0.1$ K. The data are plotted on a log-log scale and are normalized to the conductance at +50 mV.

two insulating samples 5 and 10 % above and below n_c , all at 0.1 K. This log-log-plot clearly reveals a characteristic energy scale of approximately 0.5 to 1 mV. Below ~ 0.5 mV, an obvious distinction can be made between metallic and insulating samples. The low-bias data for the metallic samples approach $V=0$ with a thermally rounded square-root shape and have a nonzero $G(V=0)$. By contrast, the insulating samples show a quasiparabolic Coulomb gap depletion of the low-energy DOS. The most important feature of Fig. 3 is that from ~ 1 to 50 mV, the conductance spectra for both metals and insulators are essentially indistinguishable. The high-bias tunneling conductance common for both insulating and metallic samples follows a functional form $G(V) \propto V^m$ where m is between 0.43 to 0.47, with no correlation of m with dopant concentration in the range of samples studied. Thus, above a characteristic energy a DOS measurement cannot differentiate between metallic and insulating states. A similar dependence was reported by Hertel *et al.*¹¹ in tunneling studies of metallic NbSi alloys near the MIT. They found that the tunneling conductance showed a square-root cusp at low energies that turned over to a slower than square-root dependence at higher energies. In NbSi m was measured to be closer to $\frac{1}{3}$.

While all the junctions used SiO₂ barriers of roughly equal thicknesses, the common high-bias conductance behavior for metals and insulators is very unlikely to be a barrier transmission artifact for two reasons. First, as we already mentioned above, the maximum bias energy is far below the SiO₂ barrier height, so that finite voltage barrier distortions are negligible. Second, this behavior is robust; it has been observed in over 25 junctions on Si:B of varying dopant densities, with junction resistances (dV/dI at +1 mV at 1.2 K) ranging from 60 to 850 k Ω over the same junction area. This order-of-magnitude variation in junction resistance is a consequence of uncontrolled variations in barrier thickness and purity. The fact that a common high-bias conductance is observed despite such differences in barrier properties indicates that the conductance form in Fig. 3 results from the DOS, not the barrier.

Figure 4 show details of the temperature dependence of the tunneling conductance for the 86 % sample from 10 to 0.5 K. Ordinary thermal broadening (i.e., broadening due

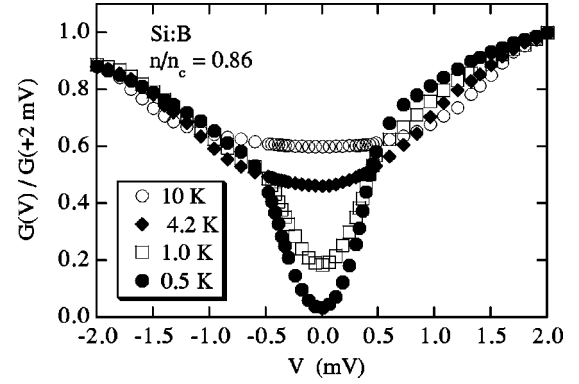


FIG. 4. Low-bias tunneling conductance-voltage spectra for the 86% Si:B sample at several different temperatures. The spectrum at each temperature is normalized to the conductance at +2 mV. Ordinary thermal broadening has not been deconvoluted.

solely to convolution with the $\partial f/\partial(eV)$ term in Eq. (2.1) has not been deconvoluted from these data. At 10 K the tunneling conductance is essentially constant within ± 1 mV of $V=0$. As temperature decreases, the opening of a roughly quadratic Coulomb gap is evident. The gap has its own temperature dependence (apart from the ordinary thermal broadening), becoming both wider and deeper as T decreases. The zero-bias DOS $N(V=0, T)$ goes approximately as T^2 at low temperature, turning over and closing [i.e., $G(0)/G(+2mV) \sim 1$] near 7 K.

III. SCALING ANSATZ FOR THE COULOMB GAP

Coulomb interactions in a disordered insulator are known to cause a correlation gap in $N(\epsilon)$. The original ES derivation⁶ for the Coulomb gap shape was given for a classical disordered system of pointlike localized electrons repelling each other via the Coulomb interaction $U(r) = e^2/\kappa r$. This derivation was based on a stability criterion for the ground state with respect to transfer of an electron from an occupied state $i(\epsilon_i < 0)$ at position r_i to an empty state $j(\epsilon_j > 0)$ at position r_j , with

$$\epsilon_j - \epsilon_i - U(r_{ij}) > 0, \quad (3.1)$$

where ϵ_i and ϵ_j are one-electron energies relative to the Fermi level. If states i and j are within energy ϵ of the Fermi level, i.e., $\epsilon_j, |\epsilon_i| < \epsilon$, then their typical separation in space $r(\epsilon) = e^2/\kappa\epsilon$ is large if ϵ is small. The DOS $N(\epsilon) \sim d[r(\epsilon)^{-3}]/d\epsilon$ then has a soft gap around $\epsilon=0$. In three dimension the result is

$$N(\epsilon) = \frac{3}{\pi} \frac{\kappa^3 \epsilon^2}{e^6}. \quad (3.2)$$

In the deep insulator, this quadratic gap extends until the noninteracting value N_0 is reached (Fig. 5). The Coulomb gap of Eq. (3.2) leads directly to the ES form for the variable-range hopping (VRH) conductivity

$$\sigma = \sigma_0 e^{-(T_0/T)^{1/2}}, \quad (3.3)$$

where

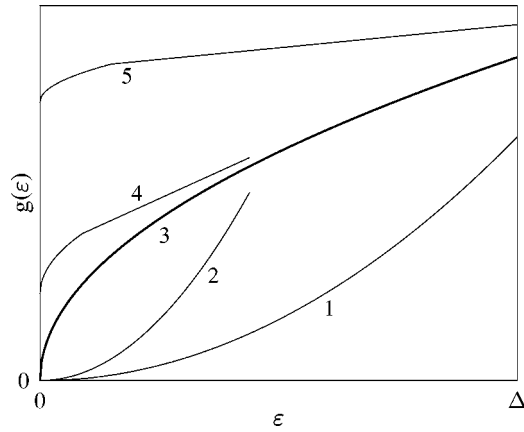


FIG. 5. Schematic plot of the DOS as a function of energy for different n : (1.) $n \leq n_c/2$, (2.) $n < n_c$ and $n_c - n \ll n_c$, (3.) $n = n_c$, (4.) $n > n_c$ and $n - n_c \ll n_c$, and (5.) $n \geq n_c/2$.

$$T_0 = C \frac{1}{k_B} \frac{e^2}{\kappa \xi}, \quad (3.4)$$

and $C \approx 2.8$ and ξ is the localization length.

The original ES theory applies to a disordered system far into the insulating side of the MIT. However, the vast majority of experimental observations of ES hopping use samples doped within 10 to 50% of n_c . Therefore, a description is required of how the Coulomb gap changes as n_c is approached from below. One can formulate a phenomenological scaling ansatz, which relates the DOS in the insulating state to other critical quantities using the ES argument. The two quantities needed to describe both disorder and Coulomb interactions near the MIT are ξ and κ . In a doped semiconductor, when $n \rightarrow n_c$ from below, ξ and κ diverge with the decreasing parameter $(1 - n/n_c)$ as

$$\xi(1 - n/n_c) = a(1 - n/n_c)^{-\nu} \quad (3.5)$$

$$\kappa(1 - n/n_c) = \kappa_0(\xi/a)^{\eta-1} = \kappa_0(1 - n/n_c)^{-\zeta}, \quad (3.6)$$

where $a = n_c^{-1/3}$ is the average distance between dopants at $n = n_c$, $\zeta = \nu(\eta - 1)$, and ν and η are scaling exponents, the same as used by McMillan.⁸ (McMillan's scaling analysis for metals does not calculate explicitly the values of these exponents but does yield the restriction $1 < \eta < 3$. Experiments³⁴ have shown that $\zeta \sim 1$.) Since κ diverges near the MIT, the Coulomb interaction becomes weaker and the Coulomb gap becomes steeper and narrower. Therefore, the VRH conductivity increases due to both the increase of the hopping rate at a given distance following Eq. (3.5), and the increase in the DOS. This is reflected in Eq. (3.4), where T_0 tends to zero as the MIT is approached from below

$$k_B T_0(n/n_c) \sim \Delta(1 - n/n_c)^{\eta\nu}, \quad (3.7)$$

where $\Delta = e^2/\kappa_0 a$. If $\eta \approx 2$ and $\nu \approx 1$, one gets $\eta\nu \approx 2$, which agrees reasonably with dc transport measurements in many materials.^{35,36} This gives important indirect evidence that the DOS is given by Eq. (3.2) with κ provided by Eq. (3.6). However, dc transport is determined entirely by a relatively small range of energies $\varepsilon \leq k_B T_0$, so that the widest possible band of energies that contribute to VRH conductiv-

ity is $k_B T_0$. Since $k_B T_0$ goes to zero near n_c , conductivity data contain no information about the DOS over a large range of energies covering

$$k_B T_0 \leq \varepsilon \leq \Delta. \quad (3.8)$$

In other words, in transport experiments we need only consider energies smaller than $k_B T_0$ or, equivalently, distances larger than ξ . Only at such distances can the hopping probability be considered exponentially small and κ be considered independent of length scale.

Tunneling spectroscopy can give direct information about the DOS in the whole range $\varepsilon \leq \Delta$, which forces us to account for interactions at distances smaller than ξ . This is accomplished by introducing spatial dispersion into κ at distances $r \ll \xi$ or, in terms of wave vector q , at $q\xi \gg 1$

$$\kappa \sim \kappa_0(r/a)^{(\eta-1)} \sim \kappa_0(qa)^{(1-\eta)} \quad (r \ll \xi). \quad (3.9)$$

At $r = \xi$ Eq. (3.9) matches Eq. (3.6), which is valid for $r \gg \xi$. Equation (3.9) means that at $r \ll \xi$

$$U(r) = \Delta(a/r)^\eta, \quad (r \ll \xi). \quad (3.10)$$

(One sees from this expression that the index η is identical to the standard dynamic scaling exponent z .)

Our goal now is to obtain the DOS throughout the energy range $k_B T_0 \leq \varepsilon \leq \Delta$ by repeating the ES argument used to derive Eq. (3.2). For $r \ll \xi$, we can use the potential in the form of Eq. (3.10) only if we create wave packets of the size r or smaller from states of the size ξ . Such a packet costs $\hbar D(r)/r^2$ of additional "localization" energy, where $D(r)$ is the diffusion coefficient at length scale r . We argue below that this energy is smaller than the energy gain per particle given by Eq. (3.10) and thus allows us to proceed with the ES argument. Using Eq. (3.1) and Eq. (3.10) we calculate an average distance $r(\varepsilon) = a(\Delta/\varepsilon)^{1/\eta}$ between electron and hole states in the band of energies of width ε around ε_F . Then using Eq. (3.2) we obtain a "critical" DOS:

$$N_c(\varepsilon) \approx a^{-3} \Delta^{-1} (\varepsilon/\Delta)^{(3/\eta)-1}. \quad (3.11)$$

At finite ξ , $N_c(\varepsilon)$ matches the quadratic part of Eq. (3.2) at $\varepsilon = k_B T_0(n)$. Thus, the width of the parabolic gap is

$$\delta \approx k_B T_0(n) \sim \Delta(1 - n/n_c)^{\eta\nu}. \quad (3.12)$$

Right at the transition (where $[1 - n/n_c] = 1/\xi = 0$) Eq. (3.11) describes the DOS at all energies $\varepsilon \leq \Delta$ (which is why we call it critical). Thus, at the very transition this scaling model has only one unknown index η . If $\eta \approx 2$, Eq. (3.11) gives $N(\varepsilon) \propto \varepsilon^{1/2}$. Critical and near-critical behavior of the DOS at $n = n_c$ is shown in Fig. 5 by a thick line. This curve plays the role of a "backbone" from which $N(\varepsilon)$ deviates down on the insulating side of the transition ($n < n_c$) and up on the metallic side ($n > n_c$) near $\varepsilon = 0$ (i.e., at distances $\gg \xi$).

Here we can connect our paper with the standard theory of quantum-phase transitions.³⁷ This theory introduces characteristic scales of length ξ and of time $\tau_\xi = \hbar/\varepsilon_\xi$, where ε_ξ is the characteristic energy. At the transition both characteristic scales diverge, so that $\tau_\xi \propto \xi^z$, where z is the dynamic scaling exponent. In our case $\varepsilon_\xi = \delta = k_B T_0(n)$ and, according to Eq. (3.12), $\tau_\xi \propto \xi^\eta$. Thus, our exponent η is the same as the standard dynamic scaling exponent z .

Until now we have proceeded from the insulating side. The behavior of the Hartree Coulomb gap on the metallic side can also be estimated in the language of the dielectric constant, wave packets, and the ES argument. At $q\xi \gg 1$ (large energies) t here is no difference between insulating and metallic phases so that Eq. (3.9) is also valid for $n > n_c$. A qualitative difference between metallic and insulating phases appears only when $q\xi \ll 1$, where instead of the scale independent κ of Eq. (3.6) one gets metallic scaling^{8,38}

$$\kappa(q) \sim \kappa_0 (a/\xi)^{(1-\eta)} (q\xi)^{-2} \quad (q\xi \ll 1) \quad (3.13)$$

This divergence of $\kappa(q)$ at small q leads to exponential screening of the interaction at distances $r \gg \xi$

$$U(r) = (e^2/\kappa_0 r) (a/\xi)^{\eta-1} \exp(-r/\xi), \quad (r \ll \xi). \quad (3.14)$$

The role of such screening was studied in Ref. 7. In the first approximation it leads to smearing of $N(\varepsilon)$ at the scale of $\delta = U(\xi) = k_B T_0$. Thus, in the metallic state $N(\varepsilon)$ becomes finite at $\varepsilon = 0$

$$N(0) = A a^{-3} \Delta^{-1} |n/n_c - 1|^{\nu(3-\eta)}, \quad (n > n_c). \quad (3.15)$$

The above expressions are all obtained in the Hartree approximation (with excluded self-interactions). In this broader sense, all these depletions of the DOS can be called Coulomb gaps. However, at very low energies in the metallic state, the Hartree approach fails and exchange interactions become dominant, leading to a square-root AA dip in the DOS near the Fermi energy.⁵ We can find the limits of the Hartree approximation if we compare the energy loss due to creation of small wave packets with the energy gain due to creation of a Coulomb gap. The first quantity is $\hbar \Delta(r)/r^2$ and the second is just ε . Their ratio

$$Q = \hbar D(r)/r^2 \varepsilon_0 = \hbar \sigma(r)/r^2 \varepsilon g(\varepsilon) e^2 = G_c / r^3 \varepsilon g(\varepsilon), \quad (3.16)$$

where $\sigma(r) = G_c e^2/\hbar$ is the conductivity in a scale r and G_c is the critical dimensionless conductance. At the very transition $r(\varepsilon) = a(\Delta/\varepsilon)^{1/\eta}$, so that Eq. (3.16) with the help of Eq. (3.2) shows that $Q \leq 1$, meaning the Hartree approximation is still reasonable. This justifies the backbone DOS Eq. (3.11) at energies $\varepsilon > \delta$ on both sides of the transition.

On the other hand, at $\varepsilon_c < \delta$ in the metallic state the Hartree approximation fails, wave packets overlap, and an AA-like theory based on exchange interactions becomes valid. As a result, a negative square root of comparable amplitude should be added to Eq. (3.15).

Now we would like to compare our results with those obtained by McMillan.⁸ In his work the Hartree interaction was neglected and the metallic side of the transition was strongly emphasized. He did not present an explicit form of low-energy behavior of DOS on the insulating side and did not mention that it is described by notion of the Coulomb gap. Nevertheless, his estimate of the ‘‘correlation gap’’ width Δ is in agreement with our width $\delta = k_B T_0$ of the parabolic Coulomb gap. In the metallic phase and in the critical regime our results are identical to those of McMillan.⁸ (Note that we use same η and ν as McMillan, but his Δ is equivalent to our $k_B T_0$ or δ .)

References 8 and 9 were criticized¹⁰ for using the single-particle DOS $N(\varepsilon)$ in the dielectric constant

$$\kappa = \kappa_0 \left[1 + \frac{4\pi N(\varepsilon) e^2}{q^2} \right]. \quad (3.17)$$

The standard expression for κ of a homogeneous system uses the thermodynamic DOS $dn/d\mu$ in place of $N(\varepsilon)$ in Eq. (3.17), where μ is the chemical potential. In an electron system with direct Coulomb interactions, $dn/d\mu$ is believed to have no gap near the Fermi level, in contrast to $N(\varepsilon)$. So which of the two DOS enters Eq. (3.17) is the crucial question. This question is directly relevant here, since all the results in this paper appear to agree with the use of Eq. (3.17). Indeed, Eqs. (3.6), (3.9), and (3.13) are self-consistently related by Eq. (3.17) to Eqs. (3.2), (3.11), and (3.15), respectively.

We can repeat the problem in terms of the screening radius r_s by rewriting Eq. (3.17) as $\kappa = \kappa_0 + 1/(r_s^2 q^2)$. If $r_s^2 = \kappa_0/4\pi N(\varepsilon) e^2$ then at small ε , $N(\varepsilon)$ is small, the radius r_s is large, the screening is weak so the interaction is strong, and finally $N(\varepsilon)$ has a Coulomb gap. For example, deep on the insulating side, using Eq. (3.2) we get that at energy ε the radius $r_s = e^2/\kappa_0 \varepsilon$, exactly equal to the average distance between states within ε of the Fermi level. This implies that screening selfconsistently does not destroy the Coulomb gap. The other option argued for in Ref. 10 starts from the DOS $dn/d\mu$. If $dn/d\mu$ is large, $r_s^2 = \kappa_0/(4\pi e^2 dn/d\mu)$ is small and we get a short-range interaction that does not lead to the Coulomb gap. This result is inconsistent with the ES argument, computer simulations, and numerous observations of the ES law for VRH conductivity. Why, then, does the conventional definition of the screening radius fail?

An answer to this question for the deeply insulating phase was suggested in Ref. 39. While the correct expression for κ contains $dn/d\mu$, in a strongly inhomogeneous system with localized states one needs a *local* κ and $dn/d\mu$ to describe the interaction of two particular states at the distance r . The local $(dn/d\mu)^{-1}$ fluctuates strongly in absolute value and has random sign. The inverse amplitude of these fluctuations equals $N(\varepsilon)$. Thus, the local screening is determined by a small random sign DOS, which in absolute value is of order $N(\varepsilon)$. The random sign of the interaction does not change any estimates based on the ES argument, and this is why the ES argument works. On the other hand, $(dn/d\mu)^{-1}$ averaged over realizations of a random potential is very small, so that the thermodynamic DOS $dn/d\mu$ is large and energy independent. The absence of self averaging in strongly disordered systems is the main reason that the *average* $dn/d\mu$ does not determine the strength of local interactions. Reference 39 discussed a classical case of a deep insulator. We assume that in the critical range of the MIT quantum effects can be taken into account by renormalization of ξ and κ and by introduction of wave packets. After that we have a problem similar to the classical one, but with renormalized interactions. This interaction for a given realization of impurities is not screened. To find $N(\varepsilon)$, one needs the local interaction and the average $dn/d\mu$ is irrelevant.

Let us remind the computer simulations lead to these conclusions.³⁹ In that work the authors considered randomly distributed pointlike donors and acceptors, all acceptors be-

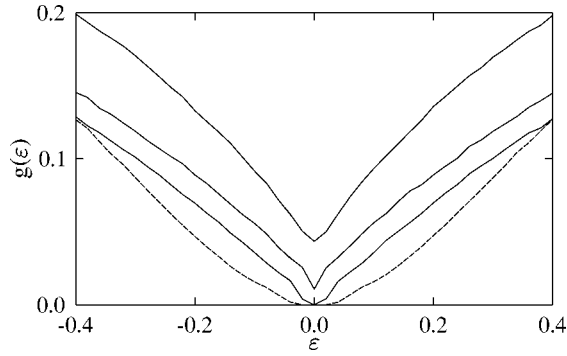


FIG. 6. DOS as a function of energy as obtained by numerical simulation for the Coulomb potential (dashed line) and for three model potentials corresponding to the critical range of the MIT (full lines) from bottom to top: $n < n_c$ ($\xi/R=2$), $n = n_c$, and $n > n_c$ ($\xi/R=2$).

ing negatively charged and some donors being occupied by electrons (and hence neutral) and others empty (and so positive). The ground state of such system is a classical realization of a Coulomb gap.^{6,7} Screening a probe positive charge at $T=0$ was studied numerically. It was shown that for a given realization of impurities, the screened potential of the probe charge is almost random in sign and its absolute value decays as $1/r$. To understand the origin of the random-sign potential for a single realization of potential, recall that in the ground-state electrons are correlated in space or, in other words, positive donors alternate with neutral ones. The probe positive charge can attract a new electron to the nearest empty donor. The positive donor left behind attracts a new electron to another of its neighbors, and so on. As a result a chain of new alternating positive and negative charges can appear. Such a chain has random direction and length and no symmetry. It is clear that the sign of the potential, for example at the end of the chain, is random. Huge cancellations appear when we average over many different realizations of impurities or over different configurations of chains. As a result spherical symmetry is restored and an exponentially small positive potential survives. This picture has been generalized for a description of the Ruderman-Kittel exchange interaction in a disordered metal.⁴⁰

An alternative explanation was recently suggested by Si and Varma,⁴¹ who argued that, contrary to previous assertions, direct Coulomb interactions do lead to a gap in the average $dn/d\mu$ when the density is low enough in a 2D system. They suggest that the incorporation of this result into the charge diffusion models of Refs. 12–14 could generate a realistic description of the transition from diffusive metal to Coulomb glass insulator.

Finally, Fig. 6 presents numerical calculations of DOS spectra of the impurity band model obtained by computer minimizations of the total energy of the system in the framework of our scaling ansatz model. To describe the MIT at $n < n_c$, $n = n_c$, and $n > n_c$, we use Coulomb potentials modified by Eqs. (3.6), (3.9), and (3.13) respectively. For concreteness, we assume $\eta=2$ and $U(r)=(R/\rho)^2$ for $n = n_c$; $U(r)=(\rho^2 + \xi^2)^{1/2}R/\rho^2$ for $n < n_c$; $U(r) = R^2/[\rho\xi(\exp \rho/\xi - 1)]$ for $n > n_c$. Here, $R = n_c^{-1/3}$ is the average distance between donors at the transition, U is measured in units of $e^2/\kappa_0 R$, and $\rho^2 = r^2 + (R/2)^2$. The $(R/2)^2$

term in the last expression is significant only at small r and is introduced as a large energy cutoff (or alternatively as a small wavelength cut-off at distances $a \sim R/2$ at n_c). The algorithm of the simulation is described in Ref. 7. The energy reference is adjusted for each realization of impurity coordinates so that the chemical potential is zero, and the DOS is averaged over 10 000 realizations. In Fig. 6, the insulating and metallic DOS are computed for states equidistant from the transition, using $\xi=2R$. We see that results of calculation are in a reasonable agreement with the schematic scaling plot of Fig. 5 and the experimental data of the previous section.

IV. ANALYSIS OF THE TUNNELING DATA

There are clearly remarkable similarities between the experimental data of Fig. 3 and the scaling ansatz results in Fig. 5. In fact, most major features of the tunneling measurements can be accounted for by the simple scaling analysis of the preceding section. It is obvious from Fig. 3 that the high-bias conductance common to both localized insulator and disordered metal plays the role of the high-energy backbone DOS obtained from the scaling ansatz by combining the dielectric constant of Eq. (3.9) with the Coulomb gap of Eq. (3.2). The distinction between metal and insulator becomes clear only when the DOS departs from the backbone at low energies. From the data, this departure occurs near an energy scale of about 0.5 meV.

While the scaling ansatz cannot calculate the value of the exponent describing the power-law backbone DOS, the experimental data does yield this number and the value of the associated scaling exponent. According to Eq. (3.10), the high-energy backbone DOS near the critical density for both metals and insulators depends on a single exponent η and should go as $N_c(\varepsilon) \propto \varepsilon^{(3/\eta)-1}$. From the data of Fig. 3, in the bias range $1 \text{ mV} \leq V \leq 50 \text{ mV}$ we obtain $G(V) \propto V^m$ with values for the exponent $m = 0.45 \pm 0.2$ covering all the samples measured. This gives $\eta = 3/(1+m) = 2.1$, which is certainly within the theoretically required bounds $1 < \eta < 3$ and in fact is essentially the same as the value $\eta=2$ reported by Hertel *et al.*¹¹ in barely metallic NbSi alloys. Since this value for η was obtained from the high-energy DOS, where metals and insulators share a common DOS character, and from many different samples both below and above n_c , we believe it is a reliable value. We do wish to emphasize that, in our interpretation, the approximately square-root behavior of the DOS at these high energies is unrelated to the AA exchange correction, which is important only at energies $\varepsilon < \delta \approx 0.4 \text{ meV}$ in the metallic state.

The exponent ν can also be examined, though less definitively than η . On the metallic side of the MIT this can be done using Eq. (3.15). The measured ratio of zero-bias conductances for the two metallic samples $G_{110}(0)/G_{105}(0) = 1.7$. Relating this conductance ratio to the ratio of the DOS and using Eq. (3.15), we obtain $\nu(3-\eta) \approx 0.77$. Taking $\eta \approx 2$ from the preceding analysis, this gives $\nu \approx 0.77$. Alternatively, ν can be estimated independently using data from the insulating samples. Figure 7 shows the measured Coulomb gap widths for four insulating samples plotted against normalized dopant density. The data fit a linear function very well with nearly zero intercept, i.e., $\delta(n) \propto (1 - n/n_c)^\gamma$ where

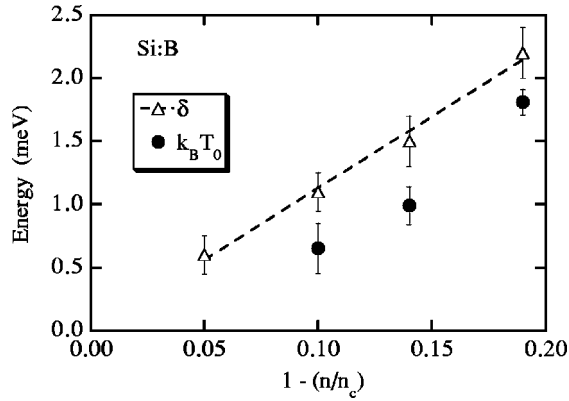


FIG. 7. Full width δ of the parabolic Coulomb gap in four insulating samples plotted against $(1 - n/n_c)$. The dashed line is a linear fit.

$\gamma \approx 1.0$. From Eq. (3.12), we have $\gamma = \eta\nu$, so that if $\eta = 2$, then the gap width data imply that $\nu = 0.5$. Figure 7 also shows that, in agreement with Eq. (3.12), the values of T_0 measured from dc conductivity in the more insulating samples, where the ES hopping law is followed most rigorously, are of the same order as the corresponding values of δ .

These values for ν obtained from the tunneling data can be compared to the independent data for $\kappa(n)$ shown in Fig. 1. A simple power-law fit to the data in that figure gives $\zeta = \nu(\eta - 1) \approx 0.71$. Thus, if η is taken to be 2 in accordance with the DOS data, then $\nu \approx 0.71$. This value is comparable to the values obtained from the DOS data analysis. Therefore, we conclude that the DOS data support values for the scaling exponents of $\eta \approx 2$ and ν somewhere between 0.5 and 0.8, at least within the range of n/n_c covered by the samples used. By way of comparison, in an insulating Si:P crystal stress tuned to within 1% of n_c , Ref. 25 found definite critical scaling of the dielectric constant in the $T \rightarrow 0$ limit with $\zeta \approx 1.0$.

The exponent ν is commonly measured by examining the very low-temperature dc conductivity $\sigma(T \rightarrow 0)$ as a function of doping and fitting the data to the form $\sigma(0) \sim (n - n_c)^\nu$ for n slightly above n_c . For nominally uncompensated doped silicon (Si:B,²⁸ Si:P,⁴² and Si:As⁴³), many such transport experiments have reported values for ν between 0.5 and 1, generally closer to 0.5 than to the $\nu \approx 1$ observed in most other disordered conductors and expected theoretically. In Si:B, for example, the exhaustive very low-temperature dc conductivity measurements reported in Ref. 28 indicate that $\nu = 0.65$. Thus our analysis of the tunneling data yield a value for ν at least consistent with that obtained from transport measurements. However, the interpretation of the transport data leading to $\nu \approx 0.5$ in Refs. 28, 42, and 43 has recently been questioned.^{44,45} There is some evidence that if only samples within $\sim 1\%$ of n_c are used, then transport measurements yield $\nu \approx 1$ instead. In fact, stress tuning of a Si:B sample⁴⁶ across the MIT has been reported to give ν as high as 1.6, although earlier stress experiments⁴⁷ on Si:P reported $\nu = 0.5$.

An estimate for the value of ξ can also be extracted from the data. Using Eq. (3.4) combined with the measured values of κ and T_0 in Figs. 1 and 7 respectively, we obtain $\xi \approx 25, 30,$ and 40 nm for the 81, 86, and 90% samples, respec-

tively. These values are in reasonable agreement with Eq. (3.5) using $\nu \sim 0.7$ and length $a = 7.5$ nm, which is close to the average distance between impurities at n_c , 6.3 nm.

It is necessary to discuss whether the scaling ansatz of Sec. III should be really applicable to the experimental situation of Sec. II. First, there is a problem with the weak compensation of the Si:B samples used. Indeed the theoretical discussion starts from the picture of a classical Coulomb gap. In the impurity band of a lightly doped semiconductor, the Coulomb gap is most pronounced for degrees of compensation (ratio of minority to majority impurity concentration) comparable to $\frac{1}{2}$. (In this case, a large number of impurities are charged, but the peak of the DOS is still not too broad.⁷) Then with increasing n the Coulomb gap evolves according to the predictions of Sec. III. In uncompensated lightly doped semiconductors, all majority impurities are occupied in the ground state and therefore are neutral. There is a large Mott-Hubbard gap that separates occupied states from empty states of a second electron on an impurity. Disorder is very weak because there are no random charges. So the Mott-Hubbard gap at the Fermi level of a lightly doped uncompensated semiconductor is a real hard gap as opposed to the soft Coulomb gap. Why then can we then talk about a Coulomb gap near the MIT? Bhatt and Rice⁴⁸ pointed out that at large impurity concentrations $n \sim n_c$ a new phenomenon that they called selfcompensation can take place. Because of large overlap and strong positional disorder of their wave functions, some clusters of impurities can have large affinity to electrons and can ionize other clusters. As a result charges will appear and a random potential will close the Mott-Hubbard gap which is already narrowed at these concentrations. Then our theory, developed for a compensated semiconductor can work even for a nominally uncompensated one. Similar tunneling experiments on compensated samples would be very important to find out whether they provide a similar DOS and whether it agrees with our theory.

A second problem is related to the role of the Al electrode in the screening of the long-range Coulomb interactions. One can think that tunneling electrons typically penetrate a distance ξ into a semiconductor. The characteristic length $r(\epsilon)$ of interactions, which determines the DOS at $\epsilon \gg \delta$ (square-root region) is smaller than ξ . This means that the large square-root region is robust with respect to screening by a metal gate. However, the parabolic gap results from the Hartree interaction between charges separated by distances $r > \xi$. Therefore, the Al electrode could produce substantial image charge screening of this interaction. Such screening was studied numerically⁴⁹ for the case of a classical Coulomb glass and a metal electrode placed directly on its surface. These computations show the bulk parabolic Coulomb gap near the surface can be closer to a linear one, rather than quadratic one. In our experiment, electrode screening may be reduced by two factors. First, the Al electrode is backed off the semiconductor surface by roughly 1.5 to 3 nm of SiO₂, as described in Sec. II. Second, the Schottky barrier between the Al and Si can be as wide as 20 nm. The cumulative effect of these two barriers is to increase the distance between the charges and image charges to distances $\sim \xi$. However, even if the gate is backed off, the parabolic gap should still be expected to fail at small enough energies. Surprisingly, the parabolic gap is more robust than expected. There is strong

agreement between the power law for the Coulomb gap as measured by tunneling and by bulk dc transport, which is not affected by electrode screening because the sample is macroscopically thick (~ 250 to $300 \mu\text{m}$) so that most of current flows far from the Al contacts. If the Coulomb gap is described by $N(\varepsilon) \sim \varepsilon^p$, then the ES model gives a hopping exponent $s = (p+1)/(p+4)$ for the conductivity $\sigma = \sigma_0 \exp\{-(T_0/T)^3\}$. For the 86% sample at 0.5 K, a power-law fit to the tunneling data gives $p = 2.2$, so the predicted ES value for $s = 0.52$. Transport measurements on the same sample in the same temperature range give a value $s = 0.51 \pm 0.02$. The close consistency of the tunneling and transport results indicates that, to a reasonable accuracy, the tunneling DOS reflects the bulk characteristics.

Finally, we should mention that the definition of DOS discussed in Sec. II does not strictly coincide with the definition of the tunneling DOS measured experimentally. Section II dealt with the bulk DOS of charged excitations (electronic polarons). For a deep insulator these excitations were introduced in Ref. 7. Electronic polarons are responsible for ES VRH. On the other hand tunneling experiments measure the one-electron DOS. For a deep insulator, a substantial difference between these two DOS in the limit of small energies was predicted in Ref. 7, but was not reliably observed in numerical simulations. We cannot resolve here this complicated problem. It may happen that this difference can explain the apparent absence of the effect of the gate on the parabolic gap. We would like only to emphasize here that this uncertainty has to do only with small energies $\varepsilon \ll \delta$ inside the parabolic Coulomb gap.

V. SUMMARY

Electron tunneling measurements of the single-particle DOS have been made on Si:B crystals ranging from 81 to

110% of the critical density of the MIT. At low energies ($\varepsilon \leq 0.5 \text{ meV}$) nonmetallic samples show an approximately quadratic soft Coulomb gap across the Fermi level, while metallic samples show a square-root cusp. At higher energies, (up to 50 meV), both insulating and metallic samples show a common DOS behavior, $N(\varepsilon) \sim \varepsilon^m$, with m slightly less than $\frac{1}{2}$. These features of the data can be understood within the framework of a scaling ansatz of the approach to the MIT from the insulating side. By extending the semiclassical Efros-Shklovskii derivation of the Hartree Coulomb gap to include a spatial dispersion of the dielectric constant at small length scales, it was shown that at short length scales ($r \ll \xi$), or high energies, spatial dispersion of κ gives rise to a common DOS that increases as a power law in both metals and insulators. This is distinct from the Altshuler-Aronov low-energy square-root cusp in the DOS arising from exchange correlations in weakly disordered metals. Only at long length scales, or, equivalently, low energies, does a quadratic Coulomb gap become apparent in insulators, while metals take on a nonzero DOS across the Fermi level. Finally, the tunneling results and the scaling ansatz suggest that a semi-classical approach may be used to treat Coulomb interaction effects on the approach to the MIT from the insulating state.

ACKNOWLEDGMENTS

We thank J. K. Wescott for help with the SiO_2 growth, and A. A. Koulakov, M. M. Fogler, and A. L. Efros for useful discussions of theoretical questions. The work at the University of Virginia was supported by NSF Grant No. DMR-9700482 and by the Research Corporation. The work at the University of Minnesota was supported by NSF Grant No. DMR-9616880

*Electronic address: marklee@virginia.edu

¹E. Abrahams, P. W. Anderson, D. C. Licciardello, and T. V. Ramakrishnan, Phys. Rev. Lett. **42**, 673 (1979).

²V. Dobrosavljevic, E. Abrahams, E. Miranda, and S. Chakravarty, Phys. Rev. Lett. **79**, 455 (1997).

³S. V. Kravchenko, W. E. Mason, G. E. Bowker, J. E. Furneaux, V. M. Pudalov, and M. D'Iorio, Phys. Rev. B **51**, 7038 (1995).

⁴S. V. Kravchenko, D. Simonian, M. P. Sarachik, W. E. Mason, and J. E. Furneaux, Phys. Rev. Lett. **77**, 4938 (1996).

⁵B. L. Altshuler and A. G. Aronov, Solid State Commun. **30**, 115 (1979); B. L. Altshuler and A. G. Aronov, Zh. Éksp. Teor. Fiz. **77**, 2025 (1979) [Sov. Phys. JETP **50**, 968 (1979)].

⁶A. L. Efros and B. I. Shklovskii, J. Phys. C **8**, L49 (1975).

⁷B. I. Shklovskii and A. L. Efros, *Electronic Properties of Doped Semiconductors* (Springer, New York, 1984)

⁸W. L. McMillan, Phys. Rev. B **24**, 2739 (1981).

⁹Y. Gefen and Y. Imry, Phys. Rev. B **28**, 3569 (1983).

¹⁰P. A. Lee, Phys. Rev. B **26**, 5882 (1982)

¹¹G. Hertel, D. J. Bishop, E. G. Spencer, J. M. Rowell, and R. C. Dynes, Phys. Rev. Lett. **50**, 743 (1983).

¹²A. M. Finkelstein, Zh. Éksp. Teor. Fiz. **84**, 168 (1983) [Sov. Phys. JETP **57**, 97 (1983)].

¹³C. Castellani, G. Kotliar, and P. A. Lee, Phys. Rev. Lett. **59**, 323 (1987).

¹⁴T. R. Kirkpatrick and D. Belitz, Phys. Rev. B **41**, 11 082 (1990).

¹⁵W. L. McMillan and J. Mochel, Phys. Rev. Lett. **46**, 556 (1981).

¹⁶Y. Imry and Z. Ovadyahu, Phys. Rev. Lett. **49**, 841 (1982).

¹⁷E. L. Wolf, D. L. Losee, D. E. Cullen, and W. D. Compton, Phys. Rev. Lett. **26**, 438 (1971).

¹⁸A. E. White, R. C. Dynes, and J. P. Garno, Phys. Rev. B **31**, 1174 (1985); Phys. Rev. Lett. **56**, 532 (1986).

¹⁹J. H. Davies and J. R. Franz, Phys. Rev. Lett. **57**, 475 (1986).

²⁰R. Rosenbaum, Phys. Rev. B **44**, 3599 (1991).

²¹D. Monroe, A. C. Gossard, J. H. English, B. Golding, W. H. Haemmerle, and M. A. Kastner, Phys. Rev. Lett. **59**, 1148 (1987).

²²J. G. Massey and Mark Lee, Phys. Rev. Lett. **75**, 4266 (1995).

²³J. G. Massey and Mark Lee, Phys. Rev. Lett. **77**, 3399 (1996).

²⁴H. B. Chan, P. I. Glicofridis, R. C. Ashoori, and M. R. Melloch, Phys. Rev. Lett. **79**, 2867 (1997).

²⁵M. A. Paalanen, T. F. Rosenbaum, G. A. Thomas, and R. N. Bhatt, Phys. Rev. Lett. **51**, 1896 (1983).

²⁶W. L. McMillan and J. M. Rowell, *Superconductivity*, edited by R. D. Parks (Dekker, New York, 1969).

²⁷W. R. Thurber, R. L. Mattis, Y. M. Liu, and J. J. Filliben, J. Electrochem. Soc. **127**, 2291 (1980).

²⁸P. Dai, Y. Zhang, and M. P. Sarachik, Phys. Rev. Lett. **66**, 1914 (1991).

- ²⁹J. G. Massey and Mark Lee, Phys. Rev. Lett. **79**, 3986 (1997).
- ³⁰T. G. Castner, N. K. Lee, G. S. Cieloszyk, and G. L. Salinger, Phys. Rev. Lett. **34**, 1627 (1975).
- ³¹T. F. Rosenbaum, R. F. Milligan, M. A. Paalanen, G. A. Thomas, R. N. Bhatt, and W. Lin, Phys. Rev. B **27**, 7509 (1983).
- ³²T. Nakanishi, S. Ohkubo, and Y. Tamura, Fujitsu Sci. Tech. J. **32**, 128 (1996).
- ³³The nonanalytic point at $V=0$ is always thermally broadened.
- ³⁴H. F. Hess, K. DeConde, T. F. Rosenbaum, and G. A. Thomas, Phys. Rev. B **25**, 5578 (1982).
- ³⁵A. G. Zabrodskii and K. N. Zinov'eva, Pis'ma Zh. Éksp. Teor. Fiz. **37**, 359 (1983) [JETP Lett. **37**, 436 (1983)].
- ³⁶J. Zhang, W. Cui, M. Juda, D. McCammon, R. L. Kelley, S. H. Moseley, C. K. Stahle, and A. E. Szymkowiak, Phys. Rev. B **48**, 2312 (1993); **57**, 4950 (1998).
- ³⁷S. L. Sondhi, S. M. Girvin, J. P. Carini, and D. Shahar, Rev. Mod. Phys. **69**, 315 (1997).
- ³⁸Y. Imry, Y. Gefen, and D. J. Bergman, Phys. Rev. B **26**, 3436 (1982).
- ³⁹S. D. Baranovskii, B. I. Shklovskii, and A. L. Efros, Zh. Éksp. Teor. Fiz. **87**, 1793 (1984) [Sov. Phys. JETP **60**, 1031 (1985)].
- ⁴⁰A. Yu. Zyuzin and B. Z. Spivak, Pis'ma Zh. Éksp. Teor. Fiz. **43**, 185 (1986) [JETP Lett. **43**, 234 (1986)].
- ⁴¹Q. Si and C. M. Varma, Phys. Rev. Lett. **81**, 4951 (1998).
- ⁴²T. F. Rosenbaum, K. Andres, G. A. Thomas, and P. A. Lee, Phys. Rev. Lett. **46**, 568 (1981).
- ⁴³W. N. Shafarman, D. W. Koon, and T. G. Castner, Phys. Rev. B **40**, 1216 (1989).
- ⁴⁴H. Stupp, M. Hornung, M. Lakner, O. Madel, and H. v. Löhneysen, Phys. Rev. Lett. **71**, 2634 (1993).
- ⁴⁵I. Shlimak, M. Kaveh, R. Ussyshkin, V. Ginodman, and L. Resnick, Phys. Rev. Lett. **77**, 1103 (1996).
- ⁴⁶S. Bogdanovich, M. P. Sarachik, and R. N. Bhatt, Phys. Rev. Lett. **82**, 137 (1999).
- ⁴⁷M. A. Paalanen, T. F. Rosenbaum, G. A. Thomas, and R. N. Bhatt, Phys. Rev. Lett. **48**, 1284 (1982).
- ⁴⁸R. N. Bhatt and T. M. Rice, Phys. Rev. B **23**, 1920 (1981).
- ⁴⁹E. Cuevas, M. Ortuño, J. Ruiz, V. Gasparian, and M. Pollak, Philos. Mag. B **70**, 1231 (1994).